We are IntechOpen, the world's leading publisher of Open Access books Built by scientists, for scientists

4,800
Open access books available

122,000
International authors and editors

135M
Downloads

Our authors are among the

154
Countries delivered to

TOP 1%
most cited scientists

12.2%
Contributors from top 500 universities

CLARIVATE ANALYTICS BOOK CITATION INDEX INDEXED

WEB OF SCIENCE™

Selection of our books indexed in the Book Citation Index in Web of Science™ Core Collection (BKCI)

Interested in publishing with us?
Contact book.department@intechopen.com

Numbers displayed above are based on latest data collected.
For more information visit www.intechopen.com

7

Conductive Adhesives as the Ultralow Cost RFID Tag Antenna Material

Cheng Yang[1, 2] and Mingyu Li[3]
[1]*Department of Mechanical Engineering*
The Hong Kong University of Science and Technology
[2]*Tsinghua University the Graduate School at Shenzhen*
[3]*School of Materials Science and Engineering*
HIT Shenzhen Graduate School
China

1. Introduction

Radio Frequency Identification (RFID) has rapidly expanded its market in recent years; until 2019, the market volume of RFID will probably reach 3.9 billion USD globally (for those passive tags). It will replace barcodes and find a lot more applications where barcodes cannot do today.[1] RFID takes the advantages such as the high-speed scanning, miniaturized size, high reliability, high memory volume, safe, and excellent read accessibility, as compared to barcodes. However, the high materials and fabrication costs are the major bottleneck for wider applications. Currently, the cost of chip is still the major part of the overall cost of a tag, which contributes about 30% to 70% of the total cost of a tag. The rest part is the sum of the materials cost including the antenna, substrate, and that for integrating them together. Since the cost of the chip keeps dropping due to the technical development, the need for reducing the other parts now is more urgent than ever. Therefore, it becomes a challenging part nowadays for reducing the cost of antenna, which takes the highest mass weight of all electrical components.

Currently, there are several alternative fabrication methods of the RFID tag antennas. For example, there are etched/punched antennas, wound antennas, which are based on metallic foils and printed antennas, which are based on the electrically conductive adhesives (ECAs). Even though each method has its pros and cons, printed antennas are currently regarded as the most promising one, primarily due to both productivity and cost concerns. Moreover, printability renders the antenna fabrication process integrated into the whole tag manufacturing system,[2] especially suitable for mass production of the RFID tags. It will also be indispensible for manufacturing the chipless tags, which eliminates the silicon chip from the tag, not only for saving cost, but there would be other benefits such as thinner in shape and more environmentally benign. However, printed RFID tags often have a shorter life-time than the etched tags (life span of more than ten years), which causes limitations in such as passports requirements; there are also concerns about the read range, which is related to the relatively low electrical conductivity. Thus there are still a lot of rooms for improvement for the printed materials.

There are a few alternative printing techniques which are applicable for printing the antenna materials (such as gravure, screen, roll to roll, flexography, and stencil etc.), which are briefly shown in Fig. 1. Here this chapter primarily elucidates the works which are based on the (flat-bed) screen printing method, which is very representative at the stage of lab prototyping. Screen printing is a low cost printing technique which has a very long history; as firstly appeared about 2000 years ago in the Qin dynasty in China. Screen printing technique uses a woven mesh to support an ink-blocking stencil. The attached stencil forms open areas of mesh that can transfer ink or other printable materials which can be pressed through the mesh as a sharp-edged image onto a substrate. A roller or squeegee is moved across the screen stencil, forcing or pumping ink to pass through the open areas in the woven mesh. There is a wide range of screen materials which include steel, polyester, glass fiber, silk fiber, and nylon etc. They form a smooth, porous, finely woven fabric which is stretched over a wood or aluminium frame. Areas of the screen are blocked off with a non-permeable material as a stencil. The open spaces of the screen allow the ink appear on the substrate beneath the screen. Generally, screen-printing method can render the printed resolution to be about 100 microns and above, which is determined by many factors such as the selection of the material of the screen mask and the automatic control of the processing conditions. The screen mask can be conveniently prepared by the ordinary photolithography method, thus it is a very promising and competitive printing method for producing the ultralow cost RFID antennas and even tags for prototyping. Moreover, screen printing can work on a large range of substrate materials such as textiles, ceramics, woods, papers, glasses, metals, and plastics. Fig. 2A shows a worker in a label printing company in Dongguan, China, whom is working on a flat-bed screen printer. The RFID tags printed in this way is shown in Fig. 2B. There were a few layers of inks including the hot-melt adhesive layer, the ECA layer, and the ink layers which were printed onto a piece of PET film consecutively. Then the printed pattern was heat-transferred onto a piece of fabric sample, which underwent dozens of washing cycles (e.g. 40 cycles) for evaluating the reliability of the sandwiched RFID tags. [3]

As the major component for the printed RFID antenna, ECAs are composed of two major parts: one is the conductive filler, such as silver, copper, and nickel; the other is the nonconductive polymer resin, which can be epoxy, polyester, polyurethane, ceramic, and other dispersants which can fit for the printing condition and some other factors. Nevertheless, high electrical conductivity of the printed antenna material is indispensible, so that the read range performance can match most of the applications of the tag.[4] Among all available printed materials including metals, carbon, and intrinsically conductive polymers, silver is considered as the most promising one, due to its high electrical conductivity (6.2×10^5 S/cm, which is the highest among all metals), relatively low material cost, and excellent reliability in long-term uses without the concern of electrochemical etches. Silver fillers are usually ground into micron-sized flakes when they are mixed with the resin dispersant; thus the overall electrical conductance of the ECA is not only determined by the intrinsic conductivity of silver, but also by the percolation effectiveness among them.[5] To improve the percolation of the silver fillers in the ECAs for practical uses, silver flakes with the diameter ranging from 30 micron to 3 micron are usually selected, which can be conveniently fabricated by mechanical machining methods such as ball-milling etc.[6] The anisotropic morphology renders the silver fillers more easily build up associated network inside the resin dispersant so that the percolation threshold (the minimum filler content requirement for achieving ohmic conductance) of the filler can be decreased.[7] Further

decreasing the size of the fillers inevitably increases the viscosity of the filler-dispersant mixture, which may cause problems during printing.

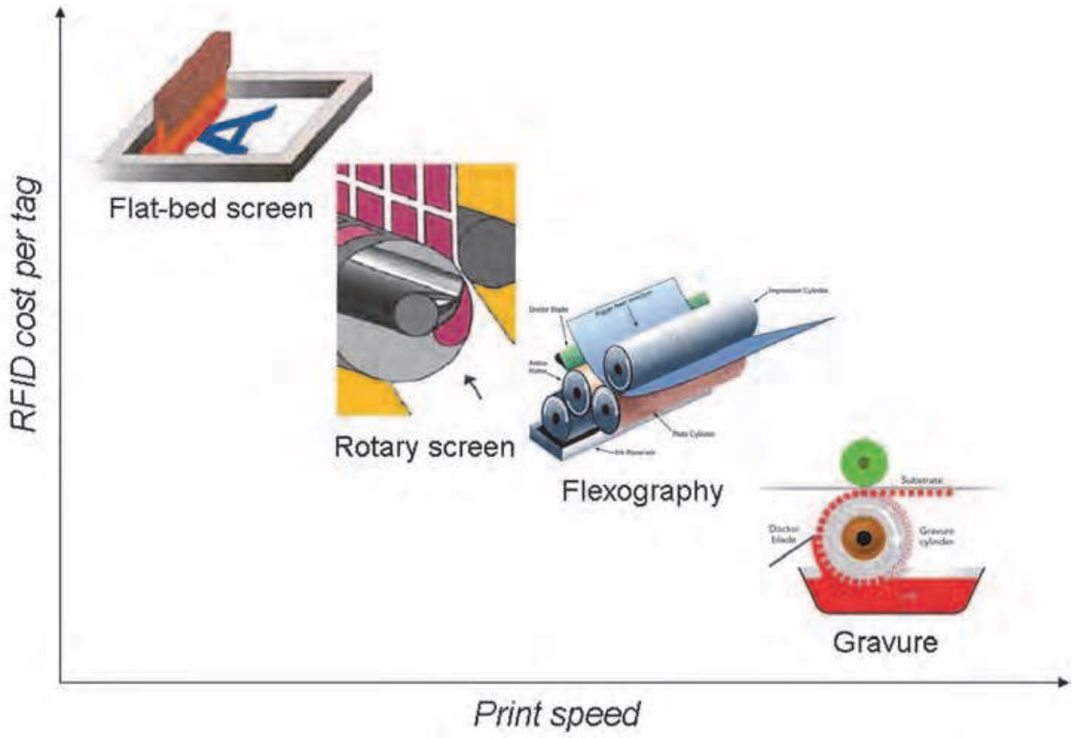

Fig. 1. A schematic comparing the printing speed and the RFID cost per tag.

Fig. 2. Photographic images showing the RFID tag incorporated high reliability hot-press labels for garments. A) A worker is screen-printing the ultralow cost ECA based antenna in his work line in a company in Dongguan, China; B) A group of labels ready for heat-transfer printing; C) Samples cotton fabric pieces with the labels heat-transferred onto them. (Upper: before washes; bottom: after washing for forty cycles.) The RFID read range performance remained the same after the heat-transfer process and the subsequent washing cycles.

There have been intensive studies about the ECAs in the last two decades,[8] majorly considered as the substitute for the Sn/Pb eutectic solders as an interconnect material in the

traditional electronic packaging industry. This is not only because they have fewer troubles about environmental problem (no lead is involved), but they have lower processing temperature and more convenient processing procedures (the curing temperature of ECAs is normally lower than the melting point of the eutectic solders, i.e. 183 ^{o}C). However, a simple mixture of the conventional resin dispersant, such as bisphenol-A type of epoxy resin and silver fillers such as microflakes (at 75% by weight) can often result in the electrical resistivity of the ECA in the range of 10^{-4} Ω ·cm. As compared to the Sn/Pb eutectic solders, the electrical conductivity of the ECAs needs to be improved to cater for general application of electrical devices.

As a noble metal, silver suffers less from the electrochemical etching problem than many others such as copper and nickel etc. However, ECAs filled by silver flakes still exhibit a high contact resistance due to a variety of factors, including the contamination from the impurities and additives of the resin dispersant (such as the free radicals from the initiator, the organic ligands from the curing agents etc.). Moreover, silver oxide exhibits a very high electrical resistivity (i.e. about 10^{16} times higher than pure silver).[9] Unlike the eutectic solders, which have a much lower melting point, the melting point of silver is 962 ^{o}C, which makes it very difficult to be annealed or sintered by conventional processing conditions. Early studies majored in those methods which can improve the physical contact among the silver fillers;[10] for example, by selecting the highly contracted resins,[10] or through applying an additional hot-laminating step after curing the ECAs.[11, 12] These strategies were shown to be able to reduce the bulk electrical resistance of the printed ECA irreversibly.[13]

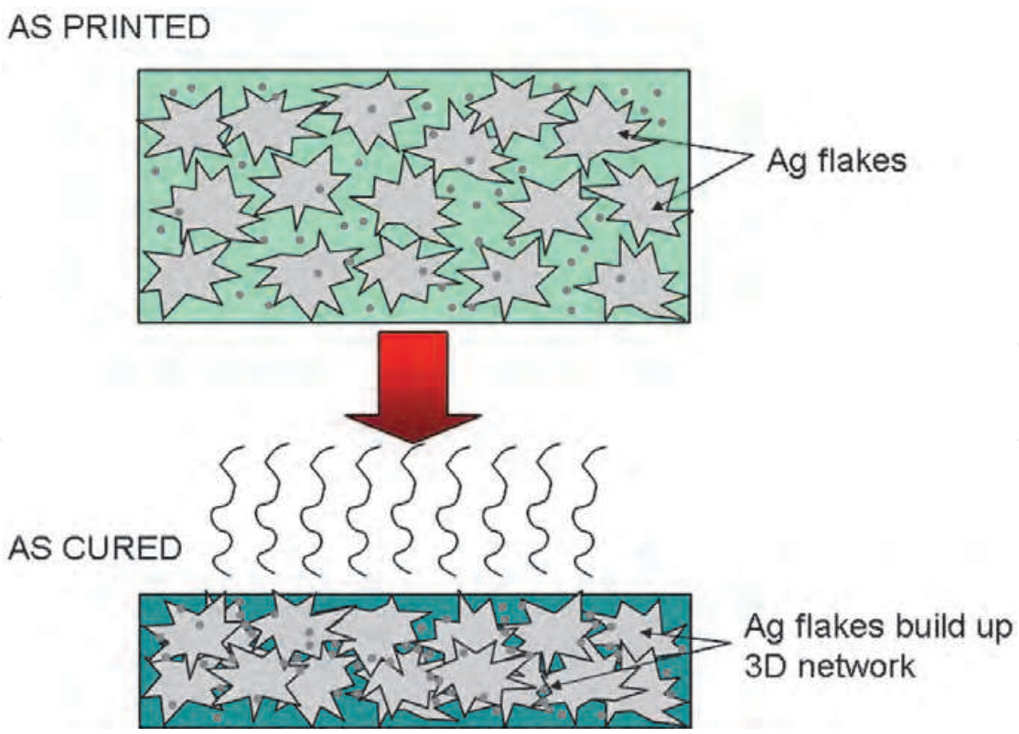

Fig. 3. A schematic showing the influence of the curing step of the ECAs, which is critical to the percolation of the fillers.

2. Recent progress of silver filler modifications

In recent years, Wong et al. conducted the researches on the self-assembled monolayer (SAM) protecting layers to the silver fillers. By seasoning a small quantity of the organic molecules (usually those which can form ligands with the metallic fillers) into the ECA formulations, the electrical resistivity of the ECAs can be drastically reduced.[14] The mechanism is rather complicated, which is supposed to be related to the red-ox process of the silver surface. Some of the SAM molecules exhibit a certain level of reducing property.[15, 16] There is a large range of the feasible compounds, including malonic acid etc., which can be used for this purpose.[15, 17, 18] On the other hand, Jiang et al. studied the effect of adding a certain ration of nano-sized silver particles to supplement the silver micro-flake fillers. By adding 40 wt% and 60 wt% of the nanosilver and microsilver, at 80 wt% filler content level, the electrical resistivity of a modified formulation can achieve ~5 x 10^{-6} Ω cm.[17] It was anticipated that the silver nanoparticles can benefit from the melting point depression effect due to the small size. Thus the silver fillers fuse with each other and build up a percolated network through ohmic contact.[19] Consequently, the electrical conductivity of the composite material approaches the lower limit of the conductive-nonconductive mixture (as shown in Fig. 3).

Yang et al. recently worked on a novel method to achieve better percolation of the silver fillers. An iodination step is applied to the silver microflakes prior to the mixing step of the ECAs, so that the electrical conductivity of the silver based ECAs can be significantly improved.[20] Silver has a strong interaction with iodine and the reaction results in the formation of silver iodide and some other compounds. Silver iodide is a semiconductive material which has indirect band-gap; the size of the silver cations is much smaller than that of iodide.[21] Silver cations can conveniently move around through the interstitial sites so as to exhibit a certain superionic conductivity.[21, 22] On the other hand, the solution-based silver microflake treatment process can eliminate the oxide layers from the silver surface.[23] After the iodination process, those iodinated regions occupy active sites such as the terraces and steps of the silver surface more selectively, and experience a subsequent ripening process,[24-27] leaving the remaining part a clean silver surface due to an electrochemical process,[26, 27] although the dynamic process still needs further investigation.

The reaction between the solid (Ag) and solute (I_2) is partially determined by the diffusion function, thus the resulting iodinated surface layer exhibits a level of nonstoichiometry. This part appears in the form of nano-islands, which are distributed on the silver flake surface. For example, TEM-EDS and SEM-EDS (Fig. 4) results both suggested that the nano-islands are distributed very sparsely on top of the silver flakes, which suggests that under optimum conditions for the best conductivity (i.e., when filled with A3) and there are excess amount of silver inside the nano-islands. The excess silver can actively involve in the charge transfer process and facilitates the reconstruction of the silver surfaces.[21]

As shown in Fig. 5A, four groups of samples were analyzed by TOF-SIMS: (1) bare silver wafer, (2) sparsely covered by the nano-islands (**1**: Ag : I = 100 : 0.2) (resembling to the surface of A3), (3) moderately covered by the nano-islands(2: Ag : I = 100 : 0.4) (resembling to the surface of A9), (4) fully iodinated surface (3: Ag : I = 100 : 20), respectively. The sum of the relative peak intensities of $^{107}Ag_2OH^+$ and $^{107}Ag_2O^+$ over that of the silver base peak ($^{107}Ag^+$) is used as the index to demonstrate the overall oxidation level of the surface. After experiencing the curing and purging processes, the surface oxidation level of the

unmodified bare silver sputtered wafer samples increased 15.5%, which suggests the oxidation of the silver surface in the curing process in the absence of Ag/AgI nanoclusters. While the surface oxidation level of the modified silver decreased 60.4% in condition **1**, and 54.3% condition **2**, respectively. This is direct evidence that the Ag/AgI nanoclusters on the silver surface prevented the silver metal surface from oxidation in curing process. But on the sample which was fully iodinated (condition **3**), the curing process incurred an increase of the total oxidation level. Since the ratio of ($^{107}Ag_2OH^+$ + $^{107}Ag_2O^+$)/$^{107}Ag^+$ is an index of the overall oxidation level of the sample surface, it appears that the less the nanoclusters covering the surface, the more fragment signals from the exposed silver metal surface were collected. For those samples with low and medium coverage levels of nanoclusters (condition 1 and 2), after curing, the overall oxidation levels were lowered by 60% and 54%, respectively. Considering the surfaces of these two samples were partially covered by the nanoclusters, after the curing process, the oxidation of the silver surface (except for the nanoclusters) was greatly inhibited. It suggests that during the curing process, the nanoclusters influence oxygen adsorption on the silver surface and recover the part of the oxidized surface. This phenomenon may be attributed to excess amount of silver in the nanoclusters, which exhibit stronger reducing property than the bulk silver substrate.[28, 29]

Fig. 5B demonstrates the situation of the silver surface when it is saturated by iodine treatment (Ag : I = 100 : 20). We tentatively partitioned the depth into two regions to facilitate the study of this spectrum: The left side illustrates the region of the nano-islands and the right side the region of the silver metal. In Fig. 5B, this ratio ($^{107}AgIO^-$/$^{107}Ag^-$) decreases with the sputtered depth, showing that the deeper the sputtering the stronger the collected substrate signals (i.e. $^{107}Ag^-$). After curing, this ratio ($^{107}AgIO^-$/$^{107}Ag^-$) increased at the sample surface which is about several nanometers in depth. For example, at the depth of ~7 nm, it is 1.1 times higher than the ratio of the sample before cure, showing that the nano-islands are further oxidized after cure. This is quite different from the TOF-SIMS analysis on a control sample of pure silver iodide crystalline powder (Aldrich, [7783-96-2], 99.999%), which shows negligible $^{107}AgIO^-$ peak intensity (ratio $AgIO^-/Ag^-$ = 6.3 ± 0.88%). As an unstable and naturally rare substance, the observation of a large quantity of silver hyperiodite ($^{107}AgIO^-$) anions in the TOF-SIMS spectra indicates that in the nanocluster regions a large amount of oxygen incorporates into the Ag/AgI nano-islands.[24, 26, 28-30] Comparison of the spectra before and after the mimic curing process demonstrates that the nano-islands are reactive to ambient oxygen and the curing process can accelerate the oxidation process. The inter-conversion between AgI and $AgIO_x$ (x = 1, 3) species has been demonstrated to be a complicated charge transfer and oxidation process which is related to many factors.[31, 32] The redistribution of the silver surface species could alter the path of oxidation of the silver surface, which may play a key role in reducing the contact resistance of the silver microflake network in the ECAs. Both the concentration and amount of iodine are crucial factors in determining the coverage and morphology of the nano-islands on the silver surface. The experimental results suggested that the coverage of these nonstoichiometric nano-islands plays a key role in modulating the surface property of silver. The ECA samples filled with A3 showed the highest electrical conductivity among all listed conditions e.g., A1, A4, A5, A6, and A9, etc., as shown in Fig. 6 (this figure only shows the resistivity data of the ECA samples lower than 10^{-3} Ω·cm). The A3 filled ECA has a volume resistivity of 5.92 x 10^{-5} Ω·cm with a silver filler content of 40 wt% (6.5 v/v%). The volume

resistivity increased to 4.81 x 10^{-4} Ω · cm when the silver filler content decreased to 27.5 wt% (3.8 v/v%). Further reduction of the filler content resulted in higher and unstable resistivity. For example, the resistivity of the ECA filled with 70 wt% of A1 is only 1.51 x 10^{-4} Ω·cm (not shown in this figure), and filled with 60 wt% of A5 is only 2.99 x 10^{-4} Ω·cm. While the resistivity of the ECA filled with 70 wt% of A3 is 6.90 x 10^{-6} Ω · cm, and filled with 60 wt% of A3 is 1.13 x 10^{-5} Ω·cm. When further decreasing the content of A3 in the ECAs to be lower than 27.5 wt%, i.e., 27 wt%, 26 wt%, 25 wt% etc., from the SEM analysis of the cross sections, sedimentations of the fillers were observed, which is due to the mismatch of the density between silver micro-flake and the epoxy resin. These sedimentations denote that when the silver filler content is lower than 27 wt%, the silver fillers can not form an associated network, which is crucial for electrical percolations. Even though this sedimentation effect may have problems in omnidirectional percolation; experimental evaluations suggest that the ultralow filler content ECAs all exhibit excellent 2D electrical conductivity in the form of printed thin film resistors.

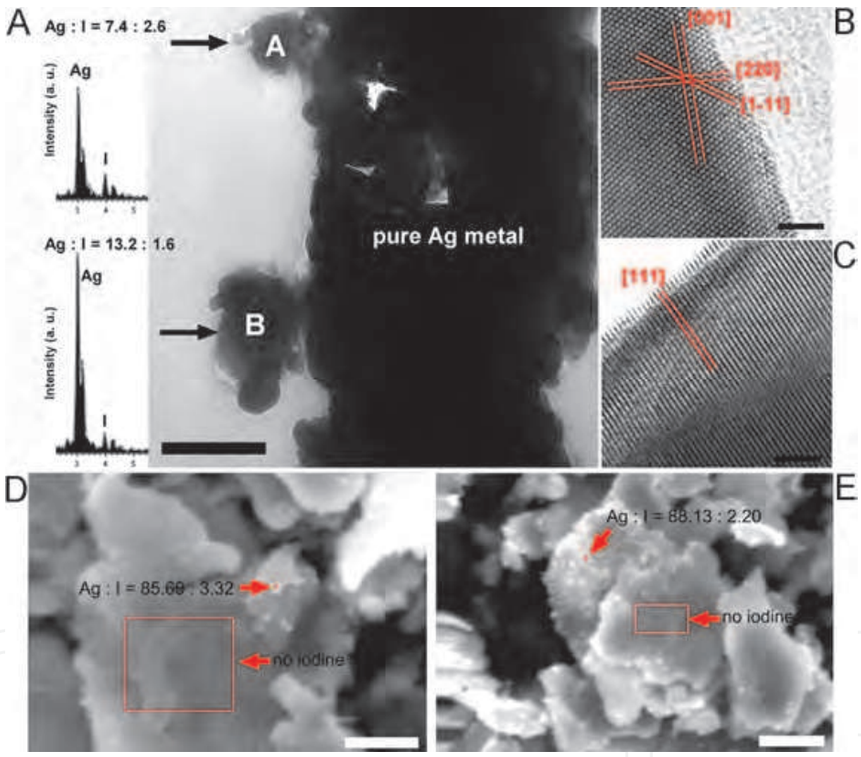

Fig. 4. A)-C): TEM-EDS analysis of the ECA cross sections. A) TEM-EDS of the nano-islands on a sectioned ECA sample (filled with A9). (Scale bar = 200 nm) EDS spectra are accompanied on the left. B) HRTEM image of bare silver micro-flake surface. (scale bar = 2 nm) C) HRTEM image of A9 filled ECA surface, except for the nanocluster parts. (scale bare = 2 nm) The crystal lattice of silver metal is marked in both the images of (b) and (c). (All samples are embedded in a resin filled with 75 wt% of the filler.) D)-E): SEM-EDS analysis of the iodinated silver flakes. D) Sample A3, the elemental ratios bentween silver and iodine are listed in this image; (scale bar = 2.5 μm) E) Sample A9, the elemental ratios bentween silver and iodine are listed in this image. (scale bar = 2.5 μm) (Copyright © 2010 WILEY-VCH)

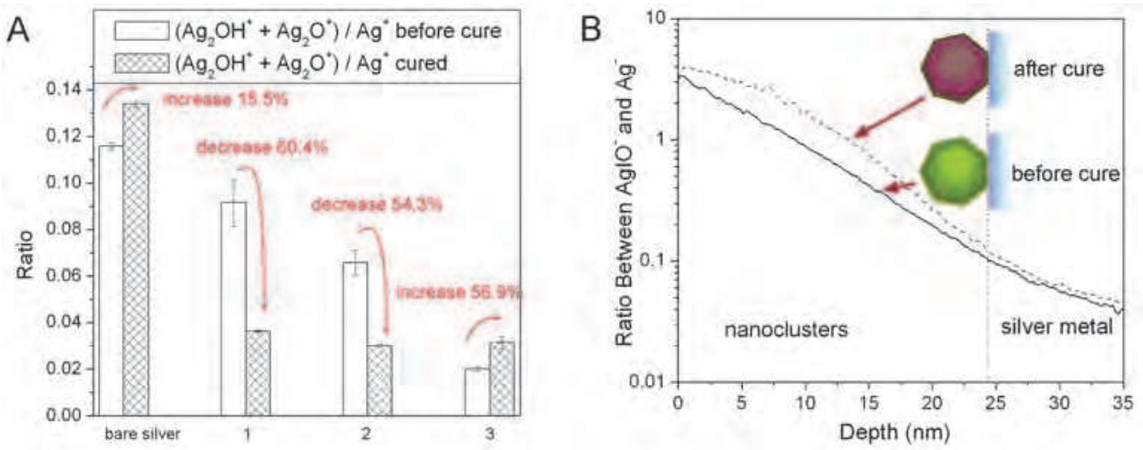

Fig. 5. TOF-SIMS analyses of the silver sputtered silicon wafer samples. A) Silver sputtered silicon wafers after treatment of different concentration of iodine solutions. (The cured samples refer to those experienced a curing and post-washing process prior to this analysis.) Conditions: 1. Ag : I = 100 : 0.2; 2. Ag : I = 100 : 0.4; 3. Ag : I = 100 : 20. B) Depth profile of the surface-modified sputtered wafer sample (treatment condition: Ag : I = 100 : 20; *y*-axis in logarithmic scale). (Copyright © 2010 WILEY-VCH)

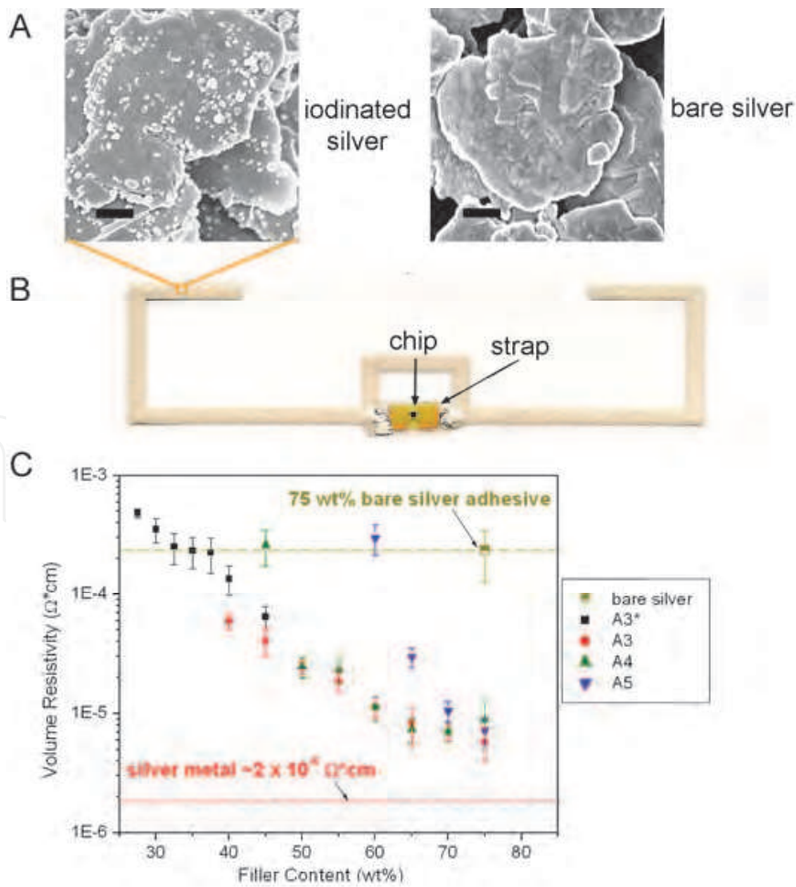

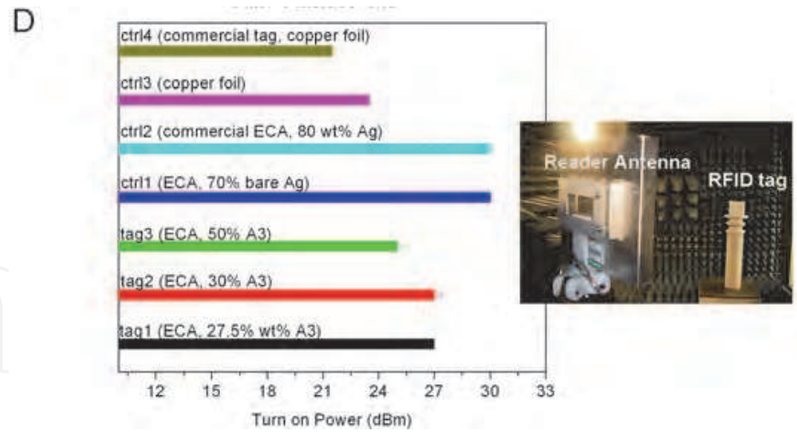

Fig. 6. A) SEM images of the iodinated silver micro-flake sample (left) and original bare silver micro-flake sample (right) (scale bar = 500 nm); B) A photographic image of a piece of UHF RFID tag using the A3-filled ECA as the antenna material. (A3, A4, and A5 are those silver fillers underwent different iodination conditions) C) The volume resistivity data of the modified ECAs with selected iodination conditions and a control bare silver-filled ECA (containing 75 wt% of silver filler). The partition lines drawn here is for comparing the resistivity of the modified ECAs versus the control silver adhesives (olive line) and silver metal (red line). (*This series of data of A3 filled ECAs are based on Novolac type epoxy resin to adjust the viscosity at low filler content.) A4: Ag : I = 0.5 : 100; A5: Ag : I = 1 : 100; D) Read range testing result of the RFID tags. Turn on power measurement on the A3 filled ECA RFID tag samples (tag 1, 2, 3) and the control samples (ctrl 1, 2, 3, 4). Except for tag2 and tag3, conformance was found when measuring all other tag samples. An EPCglobal Ultrahigh Frequency Class 1 Generation 2 RFID strap (Alien Technology Inc.) was adhered to the center of each tag antenna and the measurement was in a UHF RFID system (CSL CS461) in an anechoic chamber with a fixed reader-to-tag distance of 1 meter. Inset: A photographic image showing the turn-on power test.

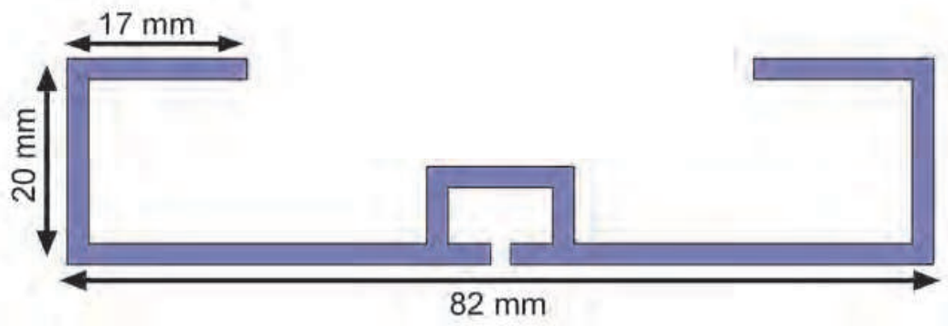

Fig. 7. Designed geometry of RFID tag antenna based on the ECA sample with 30 wt% silver.

3. Recent progress in the environmentally benign dispersants

Besides the electrical conductivity, there are also some other considerations which determine the overall performance of the ECAs. For example, the materials involved in the

printed RFID must be safe to human health and environmentally benign. This issue is especially critical to the area of food packaging and logistics at item-level. Li et al. evaluated the performance of some biocompatible curing agents to substitute the toxic curing agents for epoxy resins.[33, 34] However, the use of conventional bisphenol-A type of epoxy resin still faces lots of environmental and health problems. Yang et al. recently investigated the blocked aliphatic polyurethane (PU) as the dispersant material for preparing the ECAs for the RFID application. Two types of the methyl ethyl ketone oxime (MEKO) -blocked polyurethane prepolymers were used as they have been evaluated by the European Food Safety Authority as a safe material for food can coatings recently.[35] Moreover, as the -NCO group of the resin is blocked, the ECAs exhibit a long shelf-life than the unblocked resins. On the other hand, their moderate viscosity (1000 cPa·s to 3000 cPa·s, dependent on the amount of the silver filler content) is suitable for general screen-printing processes. Bayermaterialscience Desmodur BL 4265 SN is a kind of MEKO blocked isophorone diisocyanate (IPDI) trimer (#1) while Desmodur BL 3175 SN is a kind of MEKO blocked hexamethylene diisocyanate (HDI) trimer (#2). Both of them can couple with polyols to form low viscosity, transparent, long shelf-life paste for preparing light-stable colorless flexible, colorfast and weather-stable stoving coatings. These blocked polyurethane prepolymers are stable at room temperature when being mixed with the polyol hardener and catalyst. After mixing the dispersant with silver microflakes, the resulting ECA paste were screen-printed to PET films and cured. The structure of the blocked polyurethane prepolymers is demonstrated in scheme 1.

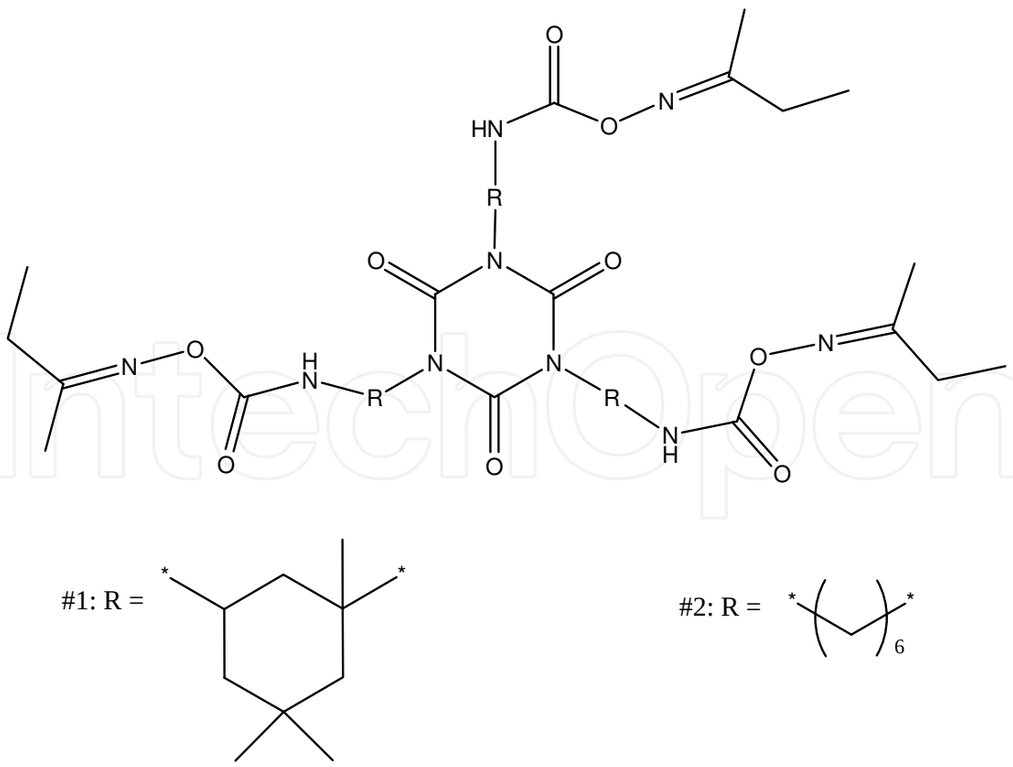

Scheme 1. Structure of the blocked polyurethane prepolymers #1 and #2: (Copyright @ 2011 Springer Publishing House)

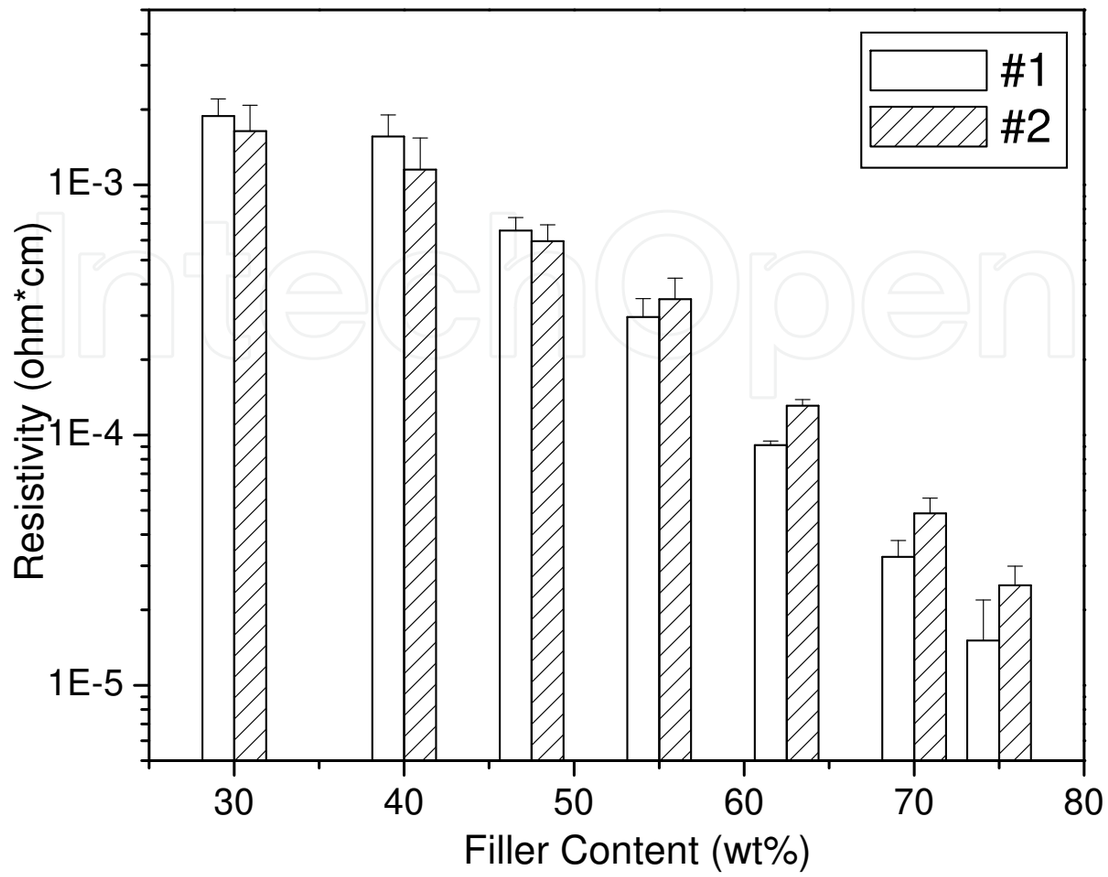

Fig. 8. Resistivity of the printed resistor of the ECAs (#1 and #2) with different silver filler contents. (Copyright @ 2011 Springer Publishing House)

Fig. 8 illustrates the electrical resistivity of the ECA antenna samples containing different silver contents (from 30 wt% to 75 wt%), which displays a series of optional conditions for the aimed cost-effectiveness. Here we can observe that with different content of silver fillers, the electrical resistivity of the ECAs varies in a range from about 2 x 10^{-5} Ω·cm to 2 x 10^{-3} Ω·cm. [3] When the silver content is lowered down to 40% and 30%, we observed that the resistivity reaches a plateau. This chart suggests that the conductivity of the PU based ECAs is comparable to those ECAs based on bisphenol-A epoxy, thus they are useful to general applications.

Fig. 9A and 9B show the changes of resistivity versus the aging time in a TERCHY MHU-150L humidity chamber (85°C/85%RH) for up to 720 hours of the two series of ECA samples. From these figures, we can observe that after the aging test, most of the electrical resistances are even lower than those before aging. For the ECA samples with relatively low filler content (30% and 40% of the filler content), the resistance even dropped about 20%. For the other samples, the variation of the resistance value is smaller than 10%, which suggest that these PU based ECAs having superior reliability up to 720 hours in their electrical conductivity.

From the SEM analysis (Fig. 11) of the cross sections of the ECA samples, we can observe that disregarding the variation of the silver content (e.g. from 30 wt% to 75 wt%), the silver

microflakes can be homogeneously distributed in the PU dispersant. In order to evaluate the performance of the PU-dispersed ECA in high frequency applications, we conducted the read range examination of the ECA printed RFID tag antennas.

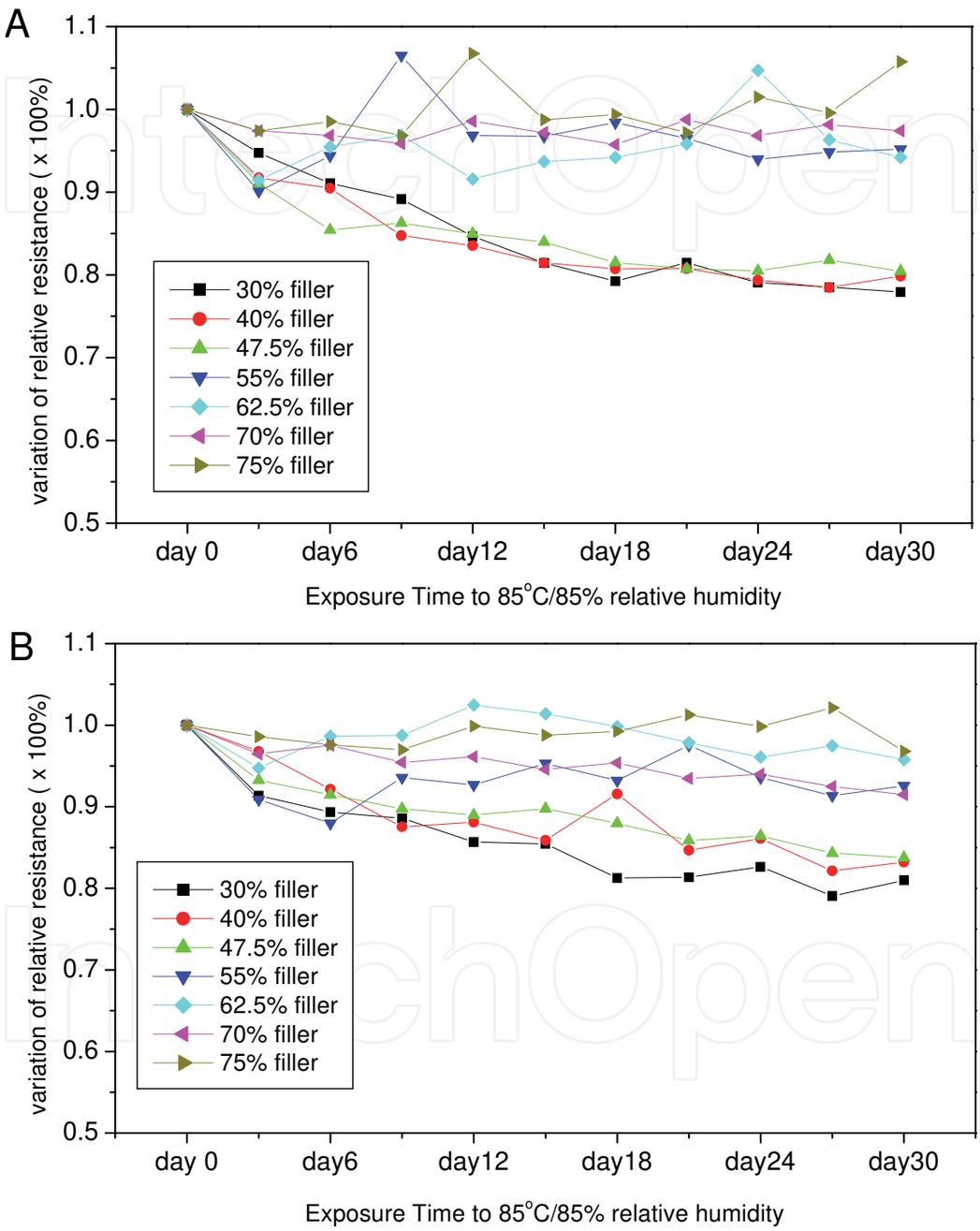

Fig. 9. Reliability analysis (85°C/85% relative humidity) of the ECAs. A) Variation of the relative resistance of the printed resistors of the ECA #1; B) variation of the relative resistance of the printed resistors of the ECA #2. . (Copyright @ 2011 Springer Publishing House)

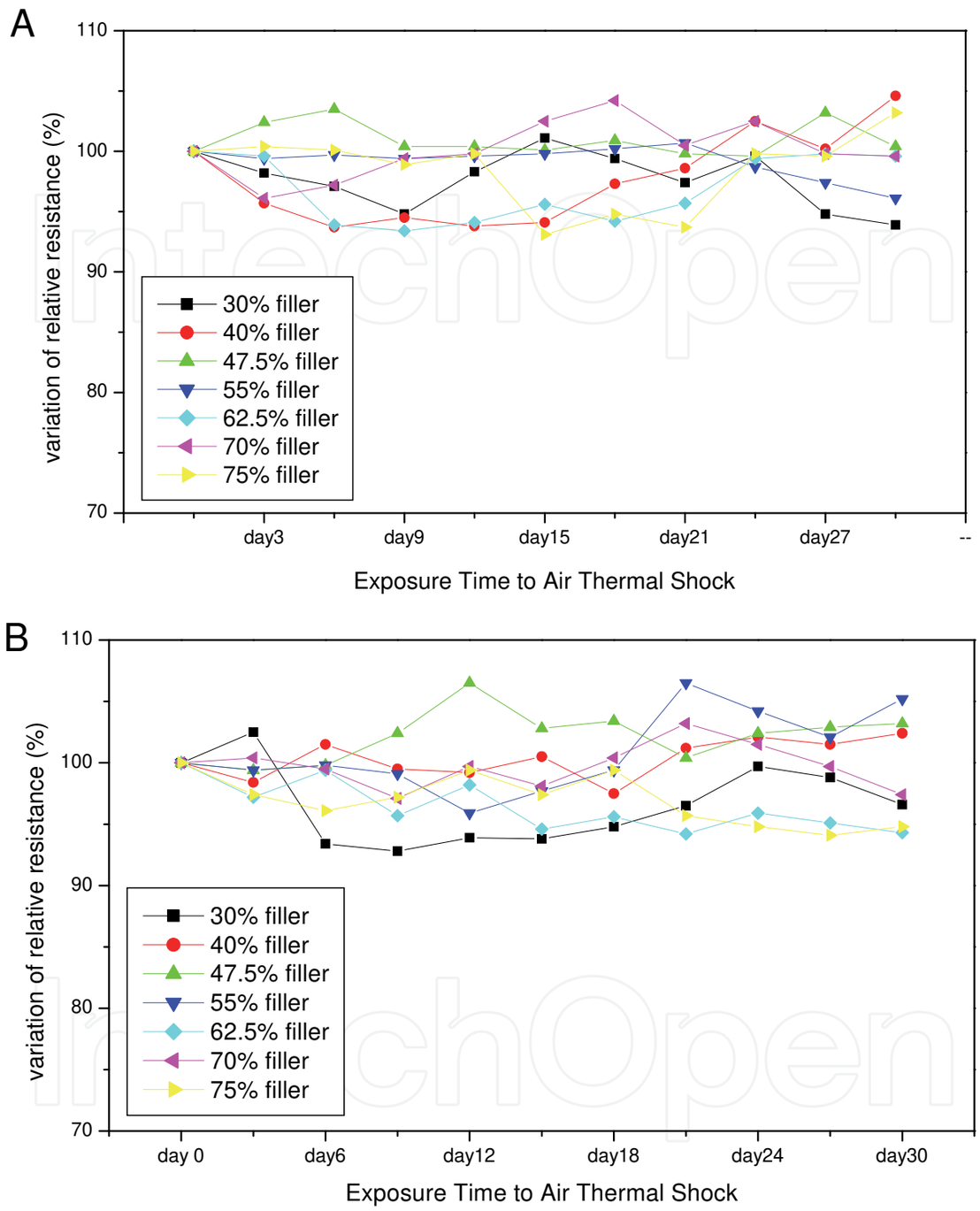

Fig. 10. Thermal cycling analysis of the ECAs. A) Variation of the relative resistance of the printed resistors of the ECA #1; B) Variation of the relative resistance of the printed resistors of the ECA #2. (Copyright @ 2011 Springer Publishing House)

Usually, the RFID antenna is designed based on the dipole antenna which is about half wavelength in length, as demonstrated in Fig. 8. Since the passive tag where the power is obtained solely from the received electromagnetic wave, the tag antenna must match the tag

circuit to maximize the transfer of power into and out of it. We selected an Alien's Gen 2 RFID chip which has an impedance value of 30 - 110j Ω, so we designed the tag antenna with the impedance value of 30 + 110j Ω to conjugate match with the chip. In the simulation, we considered both the resistivity of the materials, surface roughness, and configuration of the antenna. Based on the simulation result, we designed a series of RFID tag antenna based on #1 and #2 series. The antenna is a 82 mm-long dipole with a short line connecting two parts, as shown in Fig. 9.[36] For example, the simulated impedance of the ECA antenna filled with 30 wt% of silver filler is 33 + 108j at 915 MHz which well matches the Alien's RFID strap (30 - 110j). The calculated return loss values is -24 dB, which means over 99% power is transmitted to RFID chip. We found that the -10 dB power transmission bandwidth of the antenna is 60 MHz which covers the operation frequency of North American, China, and Hong Kong standards.[37] Herein we use the minimum turn-on power of the reader as the index of the RFID tag antenna performance. The reader is located one meter in distance towards the RFID tag (a piece of EPCglobal Class 1 Gen 2 RFID Chip is adhered to the center of the antenna). From the experimental result, we can observe that the minimum turn-on power of the reader is consistent with the electrical resistivity of the ECA samples, i.e. with the increment of the resistivity of the antenna, the reader needs a higher minimum turn-on power to detect the tag (Fig. 12). Therefore, using the same antenna design, we can adjust the content of silver filler in the ECA to cater to different requirement of read range. As for the real application of RFID technique, the power out-put of the reader is often fixed to a certain value. Controlling the resistivity of the ECA can probably be a convenient way to cater to the different requirement of read range requirement. Apparently that by using the low silver filler content paste the cost of RFID tags can be dramatically reduced. Meanwhile, the environmentally benign polyurethane based ECAs take the advantage in food supply chain and medical applications etc.

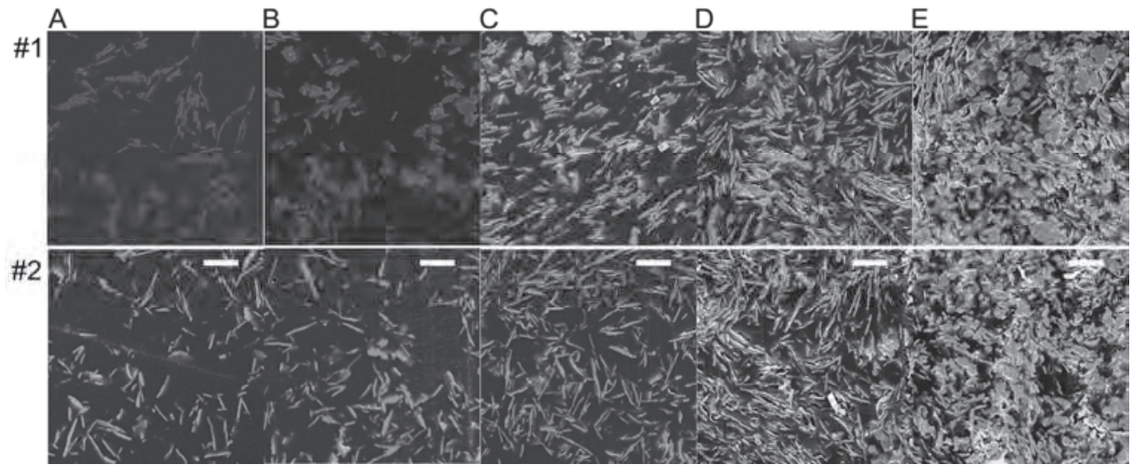

Fig. 11. SEM images of the cross sections of some of the ECA bulk samples. A) 30% of filler; B) 40% of filler; C) 55% of filler; D) 70% of filler; and E) 75% of filler. (Scale bar = 10 μm) (Copyright @ 2010 Springer Publishing House)

The ECA samples with different silver content were prepared, printed into pre-designed geometries and their performances such as electrical resistivity, adhesion strength to PET film, and high frequency performances were studied. From the experimental results, the

ECA with the silver content as low as 47.5% still maintain an acceptable conductivity (6.56 x 10^{-4} and 5.96 x 10^{-4} Ω·cm), which is efficient for high frequency applications. This suggests that by adjusting the silver content, the electrical and mechanical properties of the ECAs can be modulated. On the other hand, we observed that the silver content at 70% showed similar conductivity to those with higher silver content, which suggests that the silver content at this level reaches the summit of the conductivity. In a 720-hour 85 °C/85%RH aging test, we observed that in a large range of silver contents from 30% to 75%, the electrical resistivity of this PU based ECA was very stable. They also passed the 720-hour thermal cycling test for electrical conductivity. After all, blocked-PU based resin has been demonstrated efficient for fabricating the low-cost and flexible ECAs, which has also been demonstrated feasible in the ultra high frequency RFID tag antennas.

4. Water-based ECAs

PU displays various characters such as adjustable mechanical properties, shape-memory property, and excellent stability.[38-40] Moreover, many PU-based resins are biocompatible and can be obtained from renewable resources such as from vegetable oils.[41-43] The water-based PU resins exhibit even more advantages since there is no organic small molecule involved or released during the printing process. Recently, Yang et al. investigated the feasibility of applying the water-based PU resin as the dispersant material for the ECAs. Here cycloaliphatic PU is prepared in the emulsion based reaction. As shown in Scheme 2, the water-borne PU dispersant is prepared mainly in four steps: 1. polyether polyol (here is polytetrahydrofuran 2000), dihydroxylmethylpropionic acid (DHPA), and isophorone diisocyanate (IPDI) are mixed together for preparing the prepolymer; 2. chain extender (butylene diol) is added until the chain propagation is terminated; 3. triethylamine (TEA) is added to neutralize the system; 4. water is added dropwise so that the PU is transferred into aqueous solution. Finally, the organic solvent and the unreacted chemicals are removed by vacuum. The resulting PU emulsion is translucent bluish with long shelf-life and stable rheological property. The structure of the PU resin prepared in this way was confirmed by FT-IR spectrum. As shown in Fig. 13, the FT-IR spectrum of the dried film of the as-prepared water-borne PU is investigated. The peaks at 2933 cm^{-1} and 2854 cm^{-1} confirm the existence of the $-CH_2-$ group, the 1698 cm^{-1} the carbonyl group, and 1239 cm^{-1} and 1108 cm^{-1} confirm the C-O vibrations. The as-prepared PU has excellent thermal stability, which was confirmed by using thermalgravimetric analysis (TGA). The temperature of the sample was ramped from room temperature to 600 °C with the speed of 20 °C/min in the air (Fig. 14). The sample lost less than 10% weight before it reached 250 °C. Further raising the temperature resulted in the total decomposition, until the temperature reached 430 °C. This result suggests that the PU dispersant is suitable for the general solder reflow process as well when it is applied in the traditional packaging process.

The WBECAs were prepared by mixing the PU resin and a certain portion of the modified silver microflakes together by using a THINKY ARE250 mixer.[20] By adjusting the ratio between the two components we are able to achieve an optimum between the mechanical strength and electrical conductivity. $NaBH_4$ has been considered as a very powerful reducing agent for protecting many metals from oxidations. For example, addition of small amount of $NaBH_4$ has been demonstrated effective for improving the percolation among the copper and nickel powders via an in-situ reducing process for ink-jet printing conductive lines.[44] Here we tentatively added in 0.5% (by weight) and 1% (by weight) of $NaBH_4$ (*vs.*

Ag) into the WBECAs, as an agent for preventing the oxidation issue during the processing steps. The cross section images of the samples were studied on both transmission electron microscopy (TEM) and scanning electron microscopy (SEM). As shown in Fig. 15, the electrical resistivity of the printed resistor which is based on different silver content and $NaBH_4$ treatment condition are listed in Table 1. From Fig. 15, we can observe that the addition of $NaBH_4$ can effectively reduce the electrical resistivity of the printed resistors which were prepared by using the WBECAs. The improvement of the resistivity is about one order of magnitude.

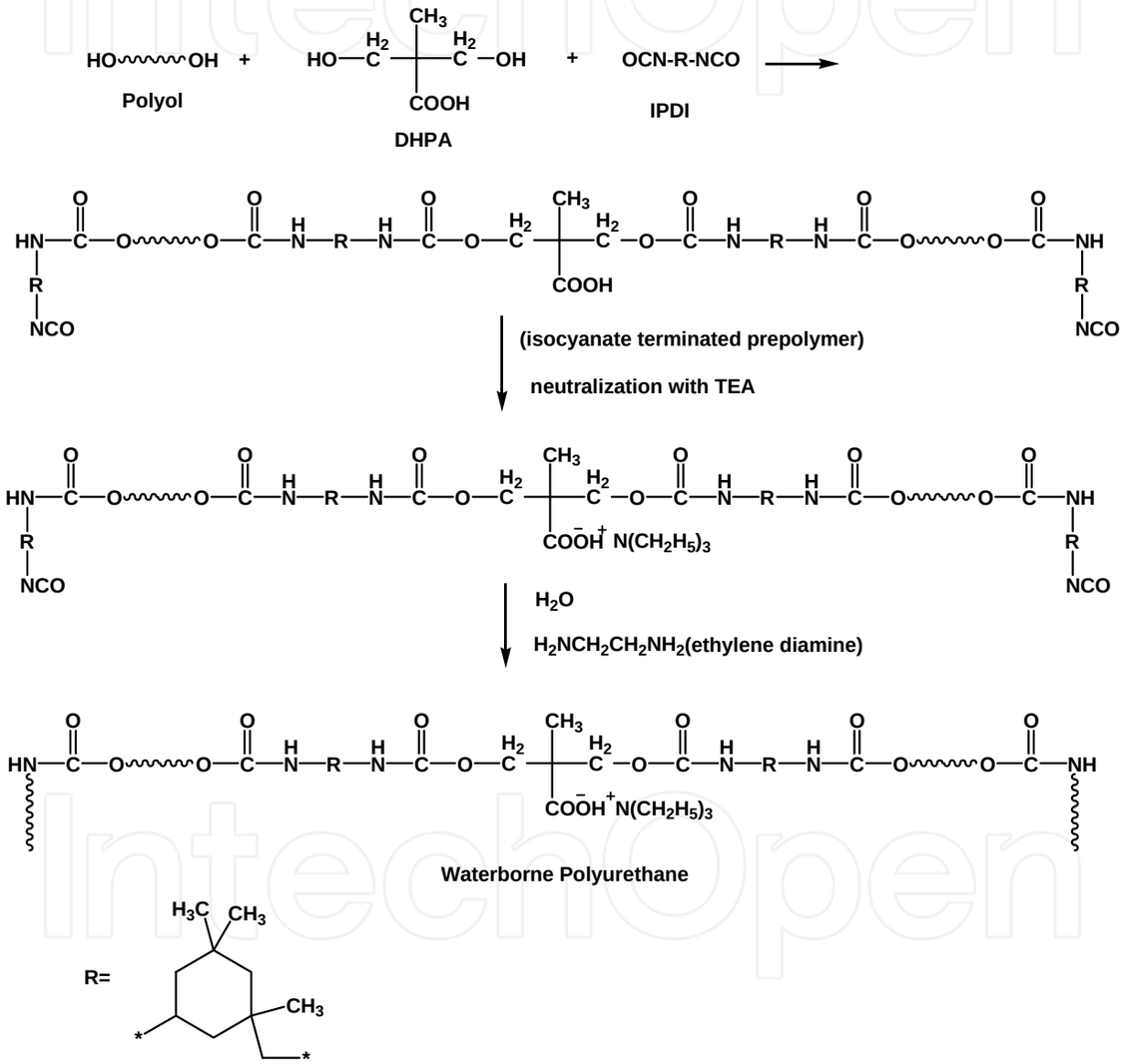

Scheme 2. Preparation route of the water-borne PU dispersant.

The measurement of the variation of electrical resistivity of the printed ECA samples were conducted in a TERCHY MHU-150L humidity chamber (85°C/85% relative humidity) for 60 days for the temperature-humidity testing (THT) (Fig. 16). As shown in Fig. 16, we can observe a trend of decrease of the electrical resistivity over the period of time. The reasons of the decrement of the electrical resistivity of all the samples are related to the following points: 1)

the water-borne PU dispersant is intrinsically an emulsion which contains both the hydrophilic part and the hydrophobic part; water molecules trapped in the interstitial sites are eliminated during the aging process or thermal curing process which renders shrinkage of the total size; 2) since the glass transition temperature (T_g) of the water-borne PU dispersant is much lower than room temperature (~-20 ^oC), the creeping of the hydrophobic polymer chain enhances the phase separation of the hydrophobic/hydrophilic regions, which results in a stronger interaction among the polymer chains by hydrophobic interaction and hydrogen bond as well. These two factors take effect both in the thermal curing process (if there is any) and the aging process as well. Thus we observed kind of variation of the electrical resistivity. After all, we did not observe any increase of the electrical resistivity of all samples after the aging test, which suggests sufficient reliability for real applications. Since many rubbery substrates are very sensitive to the high temperature (due to their extremely low T_g), they can be used as the stretchable circuit boards and fabricated at room temperature by using the WBECAs as the circuits and interconnects.

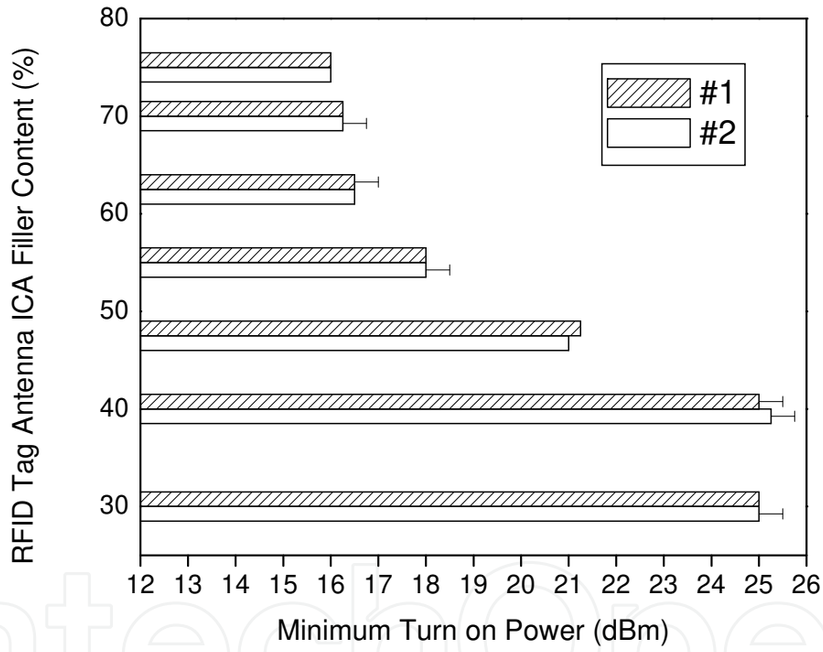

Fig. 12. Minimum turn-on power of the reader in detecting the RFID tags with the antenna printed using the ECAs. (Copyright @ 2011 Springer Publishing House)

The relation between the silver content and the tensile property of the WBECA thin film samples were investigated on an Advanced Rheometric Expansion System (ARES) (TA instruments, USA). The specimens were prepared on a piece of smooth low density polyethylene (LDPE) substrate, so that they could form an even and flat thin film. When they were naturally dried, they were peeled off carefully from the substrate and then cut into small strips with the dimension near 40 x 3 x 0.1 mm^3 (each was accurately confirmed by a caliper), and mounted onto ARES by a thin film tensile test fixture. The measurement was conducted at 25 ^oC with a 2000 g·cm transducer. The extension speed was 0.2 mm/s in a strain-controlled mode. As shown in Table 1, we can observe that the Young's

modulus of all the three samples does not change significantly along with the different silver content level. This suggests that the addition of $NaBH_4$ does not have significant influence to the mechanical strength of the WBECA samples.

Compared to the other traditional dispersants for the ECAs, such as epoxy, polyester, and polyacrylates etc., water-borne PU as the resin dispersant displays a few advantages: 1. the resin is dispersed in water, thus the printing process does not involves toxic volatile materials and the residues can be conveniently removed by water; 2. the PU materials can be prepared from a large variety of sources such as from plants, thus PU has better environmental benign character and adjustable mechanical strength; 3. the urethane bond is relatively strong, thus the materials have a high reliability for general electronic packaging applications; 4. the curing step for the ECAs can take place at even room temperature (of course a higher temperature may help accelerate the process) thus it saves energy; 5. the WBECAs have adjustable rheological property thus they are suitable for many types of printing process such as screen printing, gravure printing, and roll-to-roll printing etc.

In summary, by sensitizing a small amount of $NaBH_4$, the electrical conductivity of the WBECAs can be effectively improved of about one order of magnitude; the percolation threshold of the silver filler is reduced as well. The lowest electrical resistivity ever measured in this material was in the order of $10^{-5}\ \Omega \cdot cm$. The mechanical strength of the thin films of the free-standing WBECAs improves along with the PU dispersant amount. These WBECAs can be applied in the general printing process for general applications as ordinary ECAs can do, while they display many unique properties, such as amenity for processing, environmentally benign, excellent shelf-life and reliability in long-term storage and applications, water-proof, and the mechanical property can be adjusted by choosing different prepolymers.

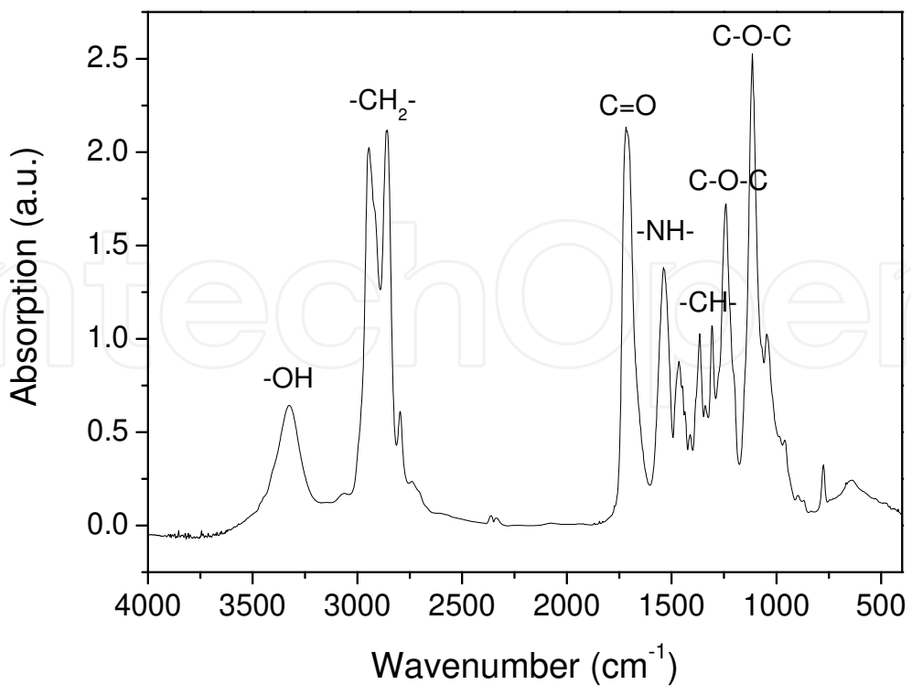

Fig. 13. FT-IR spectrum of the dried film of the water-borne PU.

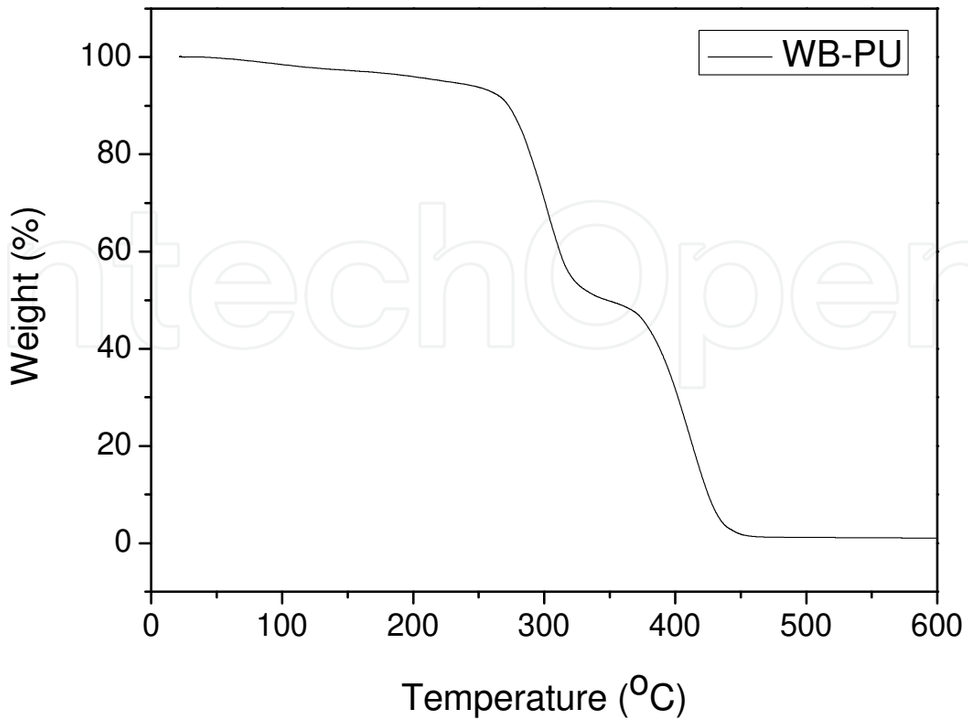

Fig. 14. TGA analysis of the PU dried film. The sample was ramped from 25 °C to 600 °C in the air.

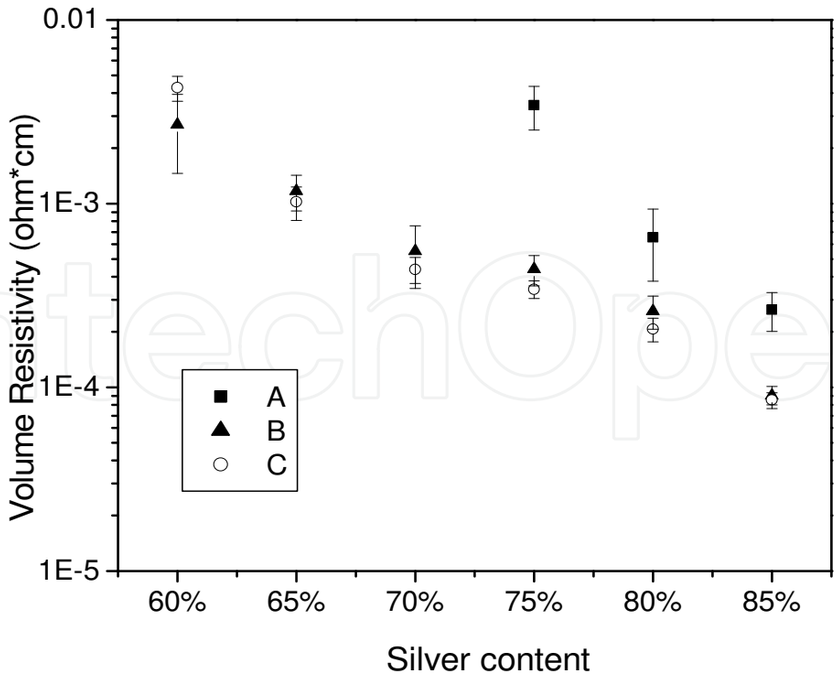

Fig. 15. Volume resistivity of the WBECAs (80 wt% of silver) versus different addition amount of $NaBH_4$. (A) no $NaBH_4$ addition; (B) 0.5% of $NaBH_4$; (C) 1% of $NaBH_4$.

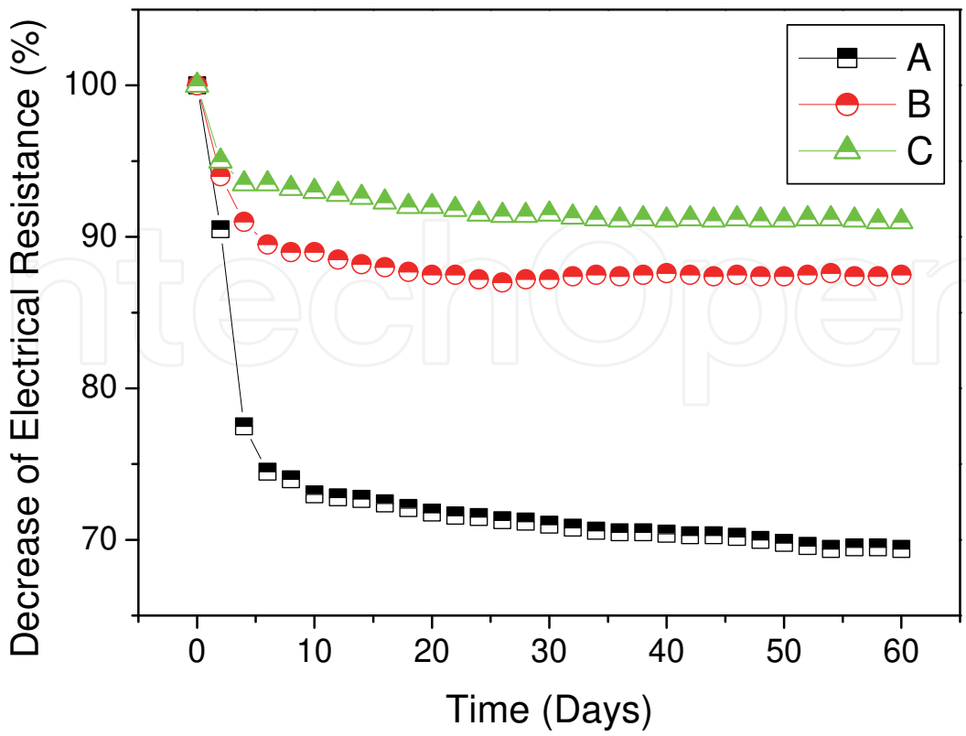

Fig. 16. Thermal-humidity reliability of the WBECAs versus aging time. (A) no $NaBH_4$ addition; (B) 0.5% of $NaBH_4$; (C) 1% of $NaBH_4$.

Young's modulus (MPa)	60% silver	70% silver	80% silver	85% silver
no treatment	0.291	0.322	0.311	0.309
0.5% $NaBH_4$	0.289	0.338	0.364	0.358
1% $NaBH_4$	0.297	0.319	0.347	0.339

Table 1. A table showing the Young's modulus of the WBECA thin film samples including the untreated, 0.5% of $NaBH_4$ treated, and 1% of $NaBH_4$ treated ones.

5. Conclusions

In summary, the authors introduced the recent progress of the silver microflake-filled ECAs as a candidate for the RFID tag antenna applications. ECAs exhibit many advantages such as printability and low-temperature processability as compared to the conventional antenna preparation methods, which render them significant in both the conventional Complementary Metal Oxide Semiconductor (CMOS) based and the organic

all-printed ones. However, their electrical, mechanical, and environmental performances are still undergoing intensive investigations. In this chapter, the authors gave several simple introductions about how to improve the electrical conductivity of the ECAs and introduced some PU based resin dispersants for ECAs. By adjusting the balance between the electrical conductivity and the materials cost, ECAs could find a larger market in both far field and near field applications. Any significant advancement of the materials would enhance the widespread uses of the tags, which is benefit from both the lower cost and higher performances. The examples given in this article have their merit and limitations; we expect that they may give elicitations for developing techniques for manufacturing low-cost, flexible ubiquitous information terminals.

6. Acknowledgement

The authors acknowledge the financial support from the Tsinghua University the Graduate School at Shenzhen.

7. References

[1] Das, R. & Harrop, P. (2009). Printed, Organic & Flexible Electronics Forecasts, Players & Opportunities 2009-2029, IDTechEx, ISBN/SKU #:IDT6769, March, 2009

[2] Finkenzeller, K. (2002). RFID-Handbuch Hanser-Verlag, ISBN 978-344-6212-78-7, München, Germany

[3] Yang, C.; Xu, B. & Yuen, M. M. F. (2008). Using Novel Materials to Enhance the Efficiency of Conductive Polymer, The 58th IEEE Electronic Components and Technology Conference, Vol. 5, pp. 213, ISBN 978-1-4244-2230-2, Orlando, Florida, USA, May 27-30, 2008

[4] Syed, A.; Demarest, K. & Deavours, D. D. (2007). Effects of Antenna Material on the Performance of UHF RFID Tags, IEEE International Conference on RFID, pp. 57-62, ISBN 1-4244-1013-4, Grapevine, TX, USA, March 26-28, 2007

[5] Stauffer, D. & Aharony, A. (1992). Introduction to Percolation Theory, Taylor & Francis ISBN 0-850-663156, London, UK

[6] Chiang, H. W.; Chung, C. L.; Chen, L. C.; Li, Y.; Wong, C. P. & Fu, S. L. (2005). Processing and shape effects on silver paste electrically conductive adhesives (ECAs), Journal of Adhesion Science and Technology, Vol. 19, No. 7, (June 2005), pp. 565-578, ISSN 0169-4243

[7] Wu, H. P.; Wu, X. J.; Ge, M. Y.; Zhang, G. Q.; Wang, Y. W. & Jiang, J. Z. (2007). Effect analysis of filler sizes on percolation threshold of isotropical conductive adhesives, Composites Science and Technology, Vol. 67, No. 6, (May 2007), pp. 1116-1120, ISSN 0266-3538

[8] Li, Y.; Moon, K. S. & Wong, C. P. (2005). Electronics without lead, Science, Vol. 308, No. 5727, (June 2005), pp. 1419-1420, ISSN 0036-8075

[9] Chatterjee, K.; Banerjee, S. & Chakravorty, D. (2004). Metal-to-insulator transition in silver nanolayers grown on silver oxide nanoparticles, Europhysics Letters, Vol. 66, No. 4, (May 2004), pp. 592-599, ISSN 0295-5075

[10] Lu, D. Q. & Wong, C. P. (2000). Effects of shrinkage on conductivity of isotropic conductive adhesives, Int. J. Adhesion & Adhesives, Vol. 20, No. 3, (May 2000), pp. 189-193, ISSN 0143-7496

[11] Kim, K. D. & Chung, D. D. L. (2005). Electrically conductive adhesive and soldered joints under compression, Journal of Adhesion Science and Technology, Vol. 19, No. 11, (November 2005), pp. 1003-1023, ISSN 0169-4243

[12] Lu, D. D.; Tong, Q. & Wong, C. P. (1999). Conductivity Mechanisms of Isotropic Conductive Adhesives (ICA's), IEEE Transactions on Electronics Packaging Manufacturing, Vol. 22, (July 1999), pp. 223-227, ISSN 1521-334X

[13] Su, B. & Qu, J. (2004) A micro-mechanics model for electrical conduction in isotropically conductive adhesives during curing, Proceedings - Electronic Components & Technology Conference, Vol. 2, (June 2004), pp. 1766-1771, ISBN: 0-7803-8365-6

[14] Li, Y.; Yim, M. J.; Moon, K. S. & Wong, C. P. (2009). Electrically conductive adhesives, Smart Materials, (November 2009), pp. 11/12, CRC Press, ISBN 978-1-4200-4372-3, Boca Raton, Fl, USA

[15] Yim, M.; Li, Y.; Moon, K. & Wong, C. P. (2007). Oxidation prevention and electrical property enhancement of copper-filled isotropically conductive adhesives, J. Elect. Mater., Vol. 36, No. 10, (August 2007), pp. 1341-1347, ISSN 1573-4803

[16] Li, Y.; Whitman, A.; Moon, K. S. & Wong, C. P. (2005). High performance electrically conductive adhesives (ECAs) modified with novel aldehydes, Proceedings - Electronic Components & Technology Conference, Vol. 2 , (May, 2005) pp. 1648-1652, ISBN 0-7803-8906-9

[17] Jiang, H. J.; Moon, K. S.; Li, Y. & Wong, C. P. (2006). Surface functionalized silver nanoparticles for ultrahigh conductive polymer composites, Chem. Mater., Vol. 18, No. 13, (May 2006), pp. 2969-2973, ISSN 0897-4756

[18] Li, Y.; Moon, K.; Whitman, A. & Wong, C. P. (2006). Enhancement of electrical properties of electrically conductive adhesives (ECAs) by using novel aldehydes, IEEE Transactions on Components and Packaging Technologies, Vol. 29, No. 4, (October 2006), pp. 758-763, ISBN 0-7803-8906-9

[19] Lu, D. D.; Li, Y. & Wong, C. P. (2008). Recent advances in nano-conductive adhesives, J. Adhes. Sci. & Tech., Vol. 22, No. 8-9, (August 2008), pp. 801-834, ISSN 0169-4243

[20] Yang, C.; Xie, Y. T.; Yuen, M. M. F.; Xu, B.; Gao, B.; Xiong, X. M. & Wong, C. P. (2010). Silver Surface Iodination for Enhancing the Conductivity of Conductive Composites, Adv. Func. Mater., Vol. 20, No. 16, (August 2010), pp. 2580-2587, ISSN 1616-301X

[21] Matsunaga, K.; Tanaka, I. & Adachi, H. (1998). Electronic mechanism of Ag-cluster formation in AgBr and AgI, Journal of the Physical Society of Japan, Vol. 67, No. 6, (December 1998), pp. 2027-2036, ISSN 0031-9015

[22] Hull, S. (2004). Superionics: crystal structures and conduction processes, Rep. Prog. Phys., Vol. 67, No. 7, (July 2004), pp. 1233-1316, ISSN 0034-4885

[23] Bardi, U. & Rovida, G. (1983). Leed, AES and Thermal Desorption Study of Iodine Chemisorption on the Silver (100), (111) and (110) Faces, Surface Science, Vol. 128, No. 2-3, (January 1983), pp. 145-168, ISSN 0039-6028

[24] Zhang, X.; Stewart, S.; Shoesmith, D. W. & Wren, J. C. (2007). Interaction of aqueous iodine species with Ag2O/Ag surfaces, J. Electrochem. Soc., Vol. 154, No. 4, (February 2007), pp. F70-F76, ISSN 0013-4651

[25] Thiel, P. A.; Shen, M.; Liu, D. J. & Evans, J. W. (2009). Coarsening of Two-Dimensional Nanoclusters on Metal Surfaces, J. Phys. Chem. C, Vol. 113, No. 13, (March 2009), pp. 5047, ISSN 1932-7447

[26] Hasse, U., Fletcher, S. & Scholz, F. (2006). Nucleation-growth kinetics of the oxidation of silver nanocrystals to silver halide crystals, J. Solid State Electrochem., Vol. 10, No. 10, (May 2006), pp. 833-840, ISSN 1432-8488

[27] Andryushechkin, B. V.; Zhidomirov, G. M.; Eltsov, K. N.; Hladchanka, Y. V. & Korlyukov, A. A. (2009). Local structure of the Ag(100) surface reacting with molecular iodine: Experimental and theoretical study, Phys. Rev. B, Vol. 80, No. 12, (September 2009), pp. 125409 1-10, ISSN 1098-0121

[28] Bonacic-Koutecky, V. & Mitric, R. (2005). Theoretical exploration of ultrafast dynamics in atomic clusters: Analysis and control, Chem. Rev., Vol. 105, No. 1, (January 2005), pp. 11-66, ISSN 0009-2665

[29] Hagen, J.; Socaciu, L. D.; Le Roux, J.; Popolan, D.; Bernhardt, T. M.; Woste, L.; Mitric, R.; Noack, H. & Bonacic-Koutecky, V. (2004). Cooperative effects in the activation of molecular oxygen by anionic silver clusters, J. Am. Chem. Soc., Vol. 126, No. 11, (February 2004), pp. 3442-3443, ISSN 0002-7863

[30] Sibbald, M. S.; Chumanov, G. & Cotton, T. M. (1997). Reductive properties of iodide-modified silver nanoparticles, J. Electroanal. Chem., Vol. 438, No. 1-2, (November 1997), pp. 179-185, ISSN 0022-0728

[31] Fourcade, F.; Tzedakis, T. & Bergel, A. (2003). Electrochemical process for metal recovery from iodized silver derivatives in liquid/solid mixture: Experimental and theoretical approaches, Chem. Eng. Sci., Vol. 58, No. 15, (August 2003), pp. 3507-3522, ISSN 0009-2509

[32] Patil, K. C.; Rao, C. N. R.; Lacksone, J. & Dryden, C. E. (1967). Silver nitrate-iodine reaction-iodine nitrate as reaction intermediate, J. Inorg. & Nucl. Chem., Vol. 29, No. 2, (February 1967), pp. 407-412, ISSN 0022-1902

[33] Li, Y.; Xiao, F.; Moon, K. & Wong, C. P. (2006). Amino acid as a novel curing agent for epoxy resins in electronic materials, PMSE Preprints, Vol. 94, pp. 873-874, ISSN 1550-6703

[34] Li, Y.; Xiao, F. & Wong, C. P. (2007). Novel, environmentally friendly crosslinking system of an epoxy using an amino acid: tryptophan-cured diglycidyl ether of bisphenol a epoxy. J. Polym. Sci. A: Polym. Chem., Vol. 45, No. 2, (January 2007), pp. 181-190, ISSN 0887-624X

[35] (2005). EFSA, Parma, Italy

[36] Chen, S. L. & Lin, K. H., Performance of a Folded Dipole with a Closed Loop for RFID Applications, in "Progress In Electromagnetics Research Symposium" (2007) pp. 329-331, ISBN 978-1-934142-01-1, Prague, Czech Republic, August 27-30, 2007

[37] Barthel, H. (2008). Regulatory status for using RFID in the UHF spectrum, EPCglobal Inc., ISBN 978-1-4244-2041-4, October 2008

[38] Subramani, S.; Park, Y. J.; Lee, Y. S. & Kim, J. H. (2003). New development of polyurethane dispersion derived from blocked aromatic diisocyanate, Prog. Org. Coat., Vol. 48, No. 1, (November 2003), pp. 71-79, ISSN 0300-9440

[39] Yang, C.; Tang, Y. H.; Lam, W. M.; Lu, W. W.; Gao, P.; Zhao, C. B. & Yuen, M. M. F. (2010). Moisture-cured elastomeric transparent UV and X-ray shielding organic-inorganic hybrids, J. Mater. Sci., Vol. 45, No. 13, (July 2010), pp. 3588-3594, ISSN 0022-2461

[40] Wicks, D. A. & Wicks, Z. W. (2001). Multistep chemistry in thin films; the challenges of blocked isocyanates, Prog. Org. Coat., Vol. 43, No. 1-3, (November 2001), pp. 131-140, ISSN 0300-9440

[41] Sharma, V. & Kundu, P. P. (2008). Condensation polymers from natural oils, Prog. Polym. Sci., Vol. 33, No. 12, (December 2008), pp. 1199-1215, ISSN 0079-6700

[42] Guner, F. S.; Yagci, Y. & Erciyes, A. T. (2006). Polymers from triglyceride oils, Prog. Polym. Sci., Vol. 31, No. 7, (July 2006), pp. 633-670, ISSN 0079-6700

[43] Petrovic, Z. S. (2008). Polyurethanes from vegetable oilsm Polym. Rev., Vol. 48, No. 1, (January 2008), pp. 109-155, ISSN 1558-3724

[44] Li, D.; Sutton, D.; Burgess, A.; Graham, D. & Calvert, P. D. (2009). Conductive copper and nickel lines via reactive inkjet printing, J. Mater. Chem. Vol. 19, (April 2009), pp. 3719-3724, ISSN 0959-9428

Current Trends and Challenges in RFID

Edited by Prof. Cornel Turcu

ISBN 978-953-307-356-9
Hard cover, 502 pages
Publisher InTech
Published online 20, July, 2011
Published in print edition July, 2011

With the increased adoption of RFID (Radio Frequency Identification) across multiple industries, new research opportunities have arisen among many academic and engineering communities who are currently interested in maximizing the practice potential of this technology and in minimizing all its potential risks. Aiming at providing an outstanding survey of recent advances in RFID technology, this book brings together interesting research results and innovative ideas from scholars and researchers worldwide. Current Trends and Challenges in RFID offers important insights into: RF/RFID Background, RFID Tag/Antennas, RFID Readers, RFID Protocols and Algorithms, RFID Applications and Solutions. Comprehensive enough, the present book is invaluable to engineers, scholars, graduate students, industrial and technology insiders, as well as engineering and technology aficionados.

How to reference

In order to correctly reference this scholarly work, feel free to copy and paste the following:

Mingyu Li and Cheng Yang (2011). Conductive Adhesives as the Ultralow Cost RFID Tag Antenna Material, Current Trends and Challenges in RFID, Prof. Cornel Turcu (Ed.), ISBN: 978-953-307-356-9, InTech, Available from: http://www.intechopen.com/books/current-trends-and-challenges-in-rfid/conductive-adhesives-as-the-ultralow-cost-rfid-tag-antenna-material

INTECH
open science | open minds

InTech Europe
University Campus STeP Ri
Slavka Krautzeka 83/A
51000 Rijeka, Croatia
Phone: +385 (51) 770 447
Fax: +385 (51) 686 166
www.intechopen.com

InTech China
Unit 405, Office Block, Hotel Equatorial Shanghai
No.65, Yan An Road (West), Shanghai, 200040, China
中国上海市延安西路65号上海国际贵都大饭店办公楼405单元
Phone: +86-21-62489820
Fax: +86-21-62489821

IntechOpen